Temperature dependence of the thermal conductivity of single-wall carbon nanotubes

To cite this article: Mohamed A Osman and Deepak Srivastava 2001 *Nanotechnology* **12** 21

INSTITUTE OF PHYSICS PUBLISHING NANOTECHNOLOGY
Nanotechnology **12** (2001) 21–24 www.iop.org/Journals/na PII: S0957-4484(01)16147-7

Temperature dependence of the thermal conductivity of single-wall carbon nanotubes

Mohamed A Osman[1,2] **and Deepak Srivastava**[3]

[1] NASA Ames Research Center, Moffett Field, CA 94035, USA
[2] School of Electrical Engineering and Computer Science, Washington State University, Pullman, WA 99164-2752, USA
[3] NASA Ames Research Center, MS T27A-1, Moffett Field, CA 94035-1000, USA

Received 7 August 2000

Abstract
The thermal conductivity of several single-wall carbon nanotubes has been calculated over a temperature range of 100–500 K using molecular dynamics simulations with the Tersoff–Brenner potential for C–C interactions. In all cases, starting from similar values at 100 K, the thermal conductivities show a peaking behaviour before falling off at higher temperatures. The peak position shifts to higher temperatures for nanotubes with larger diameters and no significant dependence on the tube chirality is observed. It is shown that this phenomenon is due to the onset of Umklapp scattering, which shifts to higher temperatures for nanotubes with larger diameters.

The discovery of carbon nanotubes (CNT) by Iijima *et al* [1–3], and subsequent observations of CNTs unique mechanical and electronic properties have initiated intensive research on these quasi-one-dimensional structures. CNTs are related to both graphite and diamond, which are known for their high thermal conductivities. Consequently, CNTs or composites based on CNTs are also proposed to be attractive for heat transport management in ULSI (ultra-large-scale integration) chips and other miniature device components due to highly directional heat flow in CNTs. Not much has been studied about the thermal conductivities of CNTs. A few recent experiments have been reported on mats of compressed ropes of CNTs [4]. By assuming that both thermal and electrical conductivities follow the same rules for transport, values of thermal conductivity of CNTs ranging from 1750 to 5850 W mK^{-1} have been extrapolated from experimental measurement on mats of nanotube ropes [4]. The experimental results, however, are difficult to interpret due to possibly deformed nanotubes and pockets of trapped voids in the mat samples.

Using molecular dynamics (MD) simulations with the Tersoff–Brenner bond order potential for C–C bonding interaction [5], we examine the temperature dependence of thermal conductivity of single-wall CNTs. A peaking behaviour in the thermal conductivity, as a function of temperature, is observed. The peak position shifts to higher temperatures for CNTs with larger diameters, while no significant dependence on tube chirality is seen. The results are explained in terms of the onset behaviour of Umklapp scattering, which lowers the thermal conductivity at higher temperatures and is strongly dependent on the nanotube radius.

The MD simulations use the Tersoff–Brenner bond-order potential [5] and solve Hamilton's classical equations of motion with a predictor–corrector algorithm with a fixed timestep of 0.5 fs. The lengths of the single-wall nanotube (SWNT) and graphene sheet are chosen to be between 151 and 221 Å, with the number of atoms ranging from 1800 to 5400. Both armchair ((5, 5), (8, 8), (10, 10), (12, 12) and (15, 15)) and zigzag (10, 0) SWNTs are simulated. The aspect ratio (length/diameter) in all the simulations is chosen to be between 10 and 20, depending on the nanotube diameter, to maintain a reasonable heat flow between the hot and cold regions of the nanotube. To simulate heat flow from a hot to a cold region, the nanotube is divided into N equal segments as shown in figure 1(a). The instantaneous temperature T_i in a segment i is determined from the kinetic energies of the atoms within the segment. The left end segment 1 is set at the temperature of a cold bath, and a hot bath is set at the middle segment at $N/2+1$ to allow the use of a periodic boundary condition along the nanotube axis [6]. The atoms in the boundary segments interact with the atoms in the rest of the tube and at equilibrium a thermal flux is maintained via energy exchange between the hot and cold regions. The heat flux in a thermally equilibrated segment is calculated according to

$$J = \frac{\langle \frac{1}{2}\sum_{k=1}^{N_B} m_k(v_k'^2 - v_k^2)\rangle}{\Delta t} \qquad (1)$$

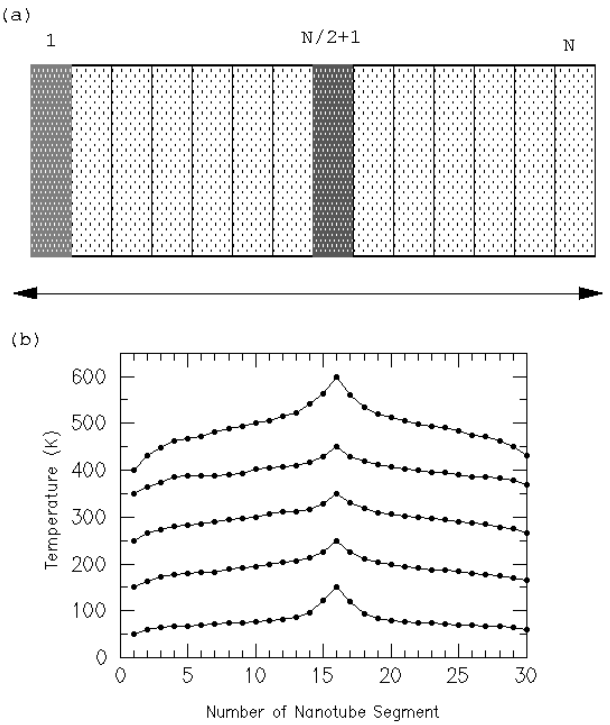

Figure 1. (*a*) Simulation system of a nanotube of a given length is divided into N equal segments with a cold bath simulated at segment 1 and a hot bath at segment $N/2+1$. (*b*) Temperature profile along a (10, 10) nanotube at (starting from the bottom) 100–500 K equilibrium temperatures.

where A is the cross-sectional area of the SWNT taken to be an annular ring of thickness 3.4 Å, Δt is the timestep taken to be 0.5 fs, and N_{B} is the number of atoms in the boundary layers. v_k and v'_k are the velocities of the atoms in the boundary layers (hot and cold slabs) before and after scaling, respectively. The equation essentially computes the change in energy per unit cross-section and divides it by the time-step to compute the flux. Figure 1(*b*) shows the final temperature distribution within a (10, 10) SWNT at five different equilibrium temperatures. The thermal conductivity κ is determined from the procedure outlined in [6].

The thermal conductivities are calculated at temperatures from 100–500 K. The thermal conductivity of (10, 10) nanotube, as shown in figure 2, increases slowly up to 300 K and then shows a peak at 400 K followed by a drop at 500 K. To see if the quantization of the phonons along the circumference was responsible for this behaviour, the calculations were repeated for a section of single layer graphene sheet with width equal to the circumference of the (10, 10) nanotube and the length the same as the nanotube. Periodic boundary conditions were applied along the width of the sheet resulting in the quantization of phonons similar to the nanotube. The calculated thermal conductivity for this sheet (figure 2), thus shows the same behaviour as that of the (10, 10) nanotube. The idea of using periodic boundary conditions on flat sections of graphene sheets to predict physical characteristics of cylindrical nanotubes is the same as that used by Benedict *et al* [7] in calculating the heat capacity of nanotubes. Moreover, the results will be significantly different if a large section of a graphene sheet without any

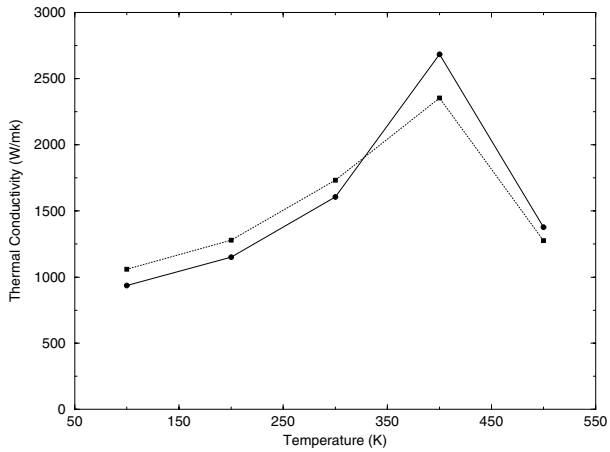

Figure 2. Thermal conductivity of a (10, 10) nanotube (solid circles) as compared with that of a single graphene layer (solid squares) containing the same number of atoms.

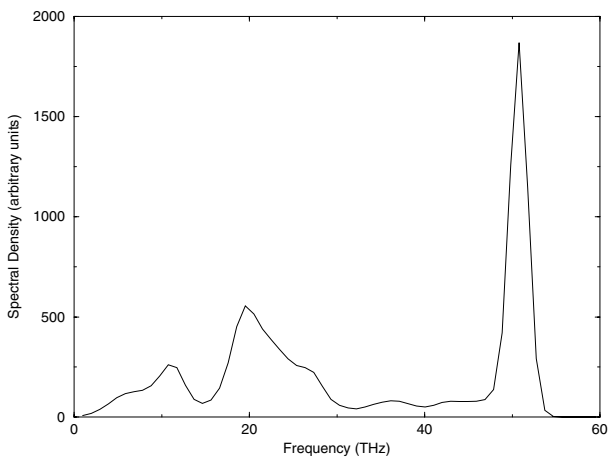

Figure 3. Phonon spectrum of the (10, 10) nanotube calculated from the Fourier transform of the velocity auto-correlation function generated during the simulations.

periodic boundary conditions along the width is used in the above simulation. A detailed investigation for the in- and out-of-plane thermal conductivity bulk graphite in comparison with that of a multi-wall nanotube is currently under investigation and will be published elsewhere [8]. The suitability of the Tersoff–Brenner potential for these simulations is checked by comparing the phonon spectrum computed using the velocity–velocity autocorrelation generated during the simulation with the experimental in-plane graphite phonon modes. The phonon spectrum for the (10, 10) nanotube, in figure 3, shows a strong peak around 50 THz which is characteristic of the graphite phonon spectrum. The broadened spectral peak at 50 THz significantly overlaps with the smaller radius dependent on the smaller peak at 28 THz due to radial enhancement in the (10, 10) nanotube. The experimentally measured in-plane thermal conductivity of pyrolytic graphite in the temperature range 100–300 K is reported to be between 500–3000 W mK^{-1} [9, 10]. Most of the reported results for SWNTs in this paper are within the experimentally measured range of in-plane thermal conductivity values.

The dependence of the thermal conductivity on the radii of nanotubes of the same chirality (armchair nanotubes) is

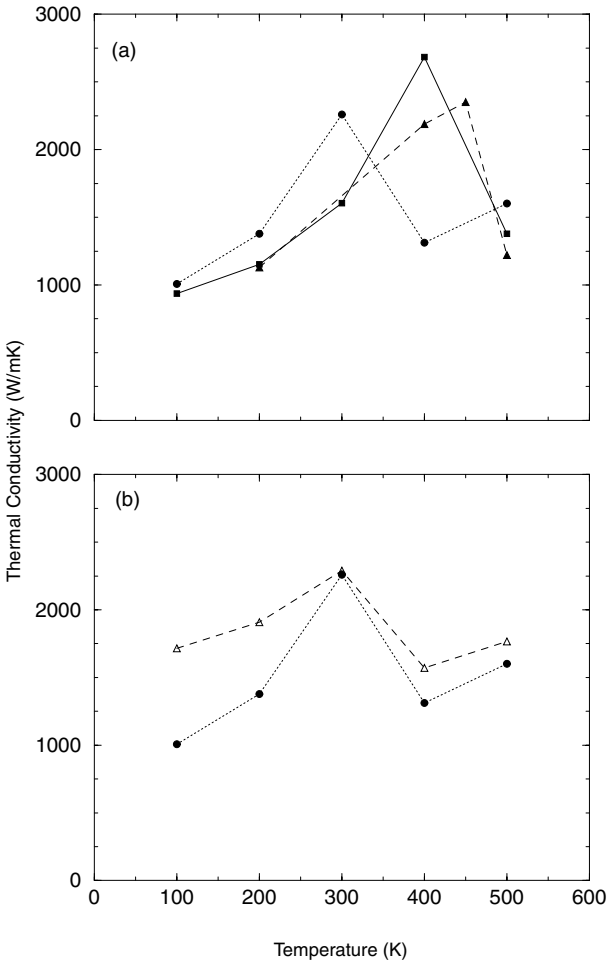

Figure 4. (*a*) Thermal conductivity of (5, 5)—solid circles; (10, 10)—solid squares; and (15, 5)—solid triangles, nanotubes of different diameters. (*b*) Thermal conductivity of (5, 5)—solid circles, and (10, 0)—open triangles, nanotubes.

shown in figure 4(*a*) for (5, 5), (10, 10) and (15, 15) nanotubes. The temperature dependence of the thermal conductivities of (8, 8) and (12, 12) nanotubes was also calculated and follows the same behaviour as described below. As shown in the figure, the values of the thermal conductivity at 100 K for all armchair SWNTs are close to each other. As the temperature is increased, the thermal conductivity increases by different rates for different tubes, up to a maximum value followed by a decrease to lower values at higher temperatures. Within the resolution of the temperature dependence reported in this paper, the peak values of the thermal conductivity of (5, 5), (10, 10) and (15, 15) SWNT occur at 300, 400, and 450 K, respectively.

The dependence of thermal conductivity on the tube chirality, via a comparison of (5, 5) and (10, 0) nanotubes, is shown in figure 4(*b*). These CNTs have the same diameter and so should not be affected by the strong diameter dependence as described above. The qualitative temperature dependence in the two cases is the same. The thermal conductivity of both peaks at 300 K. At lower temperatures, the thermal conductivity of the (5, 5) nanotube drops faster than that of the (10, 0) nanotube. This difference can be explained by the stretching strain behaviour of sigma bonds as a graphene sheet is rolled up to make a nanotube [11,12]. In armchair nanotubes the sigma bond along the circumference is strongly strained, while in zigzag nanotubes the sigma bond along the tube axis has the least strain. The excess strain along the circumference in armchair nanotubes can limit the phonon mean free path due to scattering and lower the thermal conductivity.

The diameter dependence of the peak positions of the armchair nanotubes in figure 4(*a*) is explained next. The drop in the thermal conductivity beyond its peak value is generally attributed to the increased role of resistive phonon–phonon interactions known as Umklapp processes (U-processes) [4]. In some scenario the U-processes also refer to electron–phonon scattering, we note, however, that by U-processes we refer strictly to phonon–phonon scattering processes where the final state wavevector lies outside the Brillouin zone edge. These involve large wavevector phonons and lead to $1/T$ dependence in thermal conductivity at high temperatures. In a typical U-process, randomization of the heat flow direction [13] occurs and the net heat flux along the axis is reduced. Whether the final phonon exceeds the Brillouin zone boundary or not depends on the magnitude of the phonon wavevector, i.e. axial, radial, and azimuthal components. The axial component remains independent of the tube diameter, whereas the radial and azimuthal components show strong dependence on the tube diameter. Therefore, in our discussion of the Umklapp process, we will focus on the latter two with the assumption that in a real system, simulated using the dynamic method, there is coupling between the three components and randomization of heat energy along the axial direction is possible through the excitation of U-processes along the radial and azimuthal components. We note that in model Hamiltonian based approaches this coupling is generally ignored and a complete separation of the modes within a harmonic approximation is assumed. The cyclic boundary condition around a nanotube leads to the following condition:

$$n\lambda = \pi d \tag{2}$$

where n is an integer, λ is the wavelength, and d is the nanotube diameter. The maximum allowed wavelength is obtained by setting $n = 1$ which also determines the minimum allowed wavevector $q_{\min}$ according to,

$$q_{\min} = \frac{2\pi}{\lambda_{\max}} = \frac{2}{d}. \tag{3}$$

Therefore, it follows that the minimum wavevectors vary inversely with the tube diameter. In other words, the minimum wavevectors in small diameter SWNTs are larger than those in large diameter SWNTs and closer to the reciprocal lattice vector needed for a U-process. The overall magnitude of the phonon wavevector depends on the magnitude of all three components of the wavevector. The axial component has the same distribution for all the nanotubes, however, the radial and azimuthal components tend to favour long wavevectors for small diameter nanotubes. Consequently, at any given temperature, the probability of U-processes is higher in SWNTs with smaller diameters as compared to tubes with larger diameters. Since, the U-processes cause a drop in thermal conductivity from their peak value, these peaks will occur at lower temperatures in small diameter

nanotubes. This is consistent with the results in figure 4(*a*) where thermal conductivity peaks shift to higher temperatures for CNTs of larger diameter and there is no dependence on tube chirality.

The above features in the thermal conductivity, explained due to the onset of U-processes, also indicate a dominant role of radial phonons as a mechanism for heat transport in SWNTs. The presence of strong radial phonons in both zigzag and armchair SWNTs have been described earlier by the static lattice dynamics calculations of Charlier *et al* [14] and Rao *et al* [15]. They have developed an experimentally parametrized (proportional to $1/D$) dependence of radial phonon frequency on nanotube diameters [15]. Their experimental results indicate that the frequency of radial phonons shifts to lower values for CNTs of larger diameters. This allows the thermal conductivity peaks to occur at higher temperatures for large diameter nanotubes before being suppressed by phonon–phonon scattering or U-processes.

In summary, we have investigated the temperature dependence of thermal conductivity of SWNTs near room temperature (100–500 K). The electronic contribution to the thermal conductivity in graphene sheets and CNTs, at these temperatures, is expected to be negligible due to the low density of free charge carriers [4, 16]. For example, Benedict *et al* [7] showed that phonon contribution was dominant down to 0 K and that the phonon contribution to the heat capacity was 10 000 times larger than the electronic contribution. The thermal conduction at these temperatures is found to be strongly dependent on the diameter of the nanotube with no dependence on the tube chirality. The thermal conductivity for all nanotubes exhibits a peaking behaviour as a function of temperature, and the peak position shifts to higher temperatures for larger diameter SWNTs. This behaviour is attributed to a combination of factors; the onset behaviour of Umklapp scattering; and the fact that heat is carried mainly through radial phonons. Both of these factors have strong tube radius dependence and weak or no chirality dependence.

Our simulation results, and the above discussion, demonstrate the possibility of developing specific materials for thermal transport management that could be optimized for applications in a particular temperature range. For example, (5, 5) nanotubes provide the highest thermal conductivity at room temperature, as compared to (10, 10) and (15, 15) nanotubes. A weak dependence of the temperature behaviour of the CNT thermal conductivity on their chiralities, for tubes of the same diameter, is probably desirable from an applications' perspective, since at present it is not possible to produce nanotubes of a given chirality in a controlled manner.

A precise knowledge of CNT thermal conductivity will be useful in designing efficient thermal transport management materials and devices specially suited for micro- and nano-scale applications. Our work is a first step in that direction.

Acknowledgments

We thank Dr T R Govindan, and Dr T Yamada of NASA Ames, and Dr A M Rao of the University of Kentucky for useful discussions during the development of this paper. The use of computing facilities at NAS division of NASA Ames Research Center, and the Solid State Device Animation Laboratory funded by the NSF's Division of Undergraduate Education through grant no DUE 9651416 is appreciated. This paper was done while MAO was on sabbatical leave at NASA Ames, and part of this paper (DS) is supported by CSC under NASA contract no DTTS59-99-D-00437/A61812D.

Note added. The thermal conductivity of a (10, 10) nanotube using the same Tersoff–Brenner potential [5] and a thermal current correlation function method has been recently reported by Che *et al* [17]. They calculate the thermal conductivity of a constant diameter nanotube as a function of defect and vacancy concentration, whereas our work explores the temperature dependence of the thermal conductivity as a function of tube diameter and chirality. The tube length (22 nm) used in our work for all diameters is also shown to be enough to achieve convergence in the paper of Che *et al* [17].

References

[1] Iijima S 1991 *Nature* **354** 56
[2] Iijima S and Ichihashi T 1993 *Nature* **363** 603
Bethune D S, Kiang C-H, deVries M S, Gorman G, Savoy R, Vazquez J and Beyers R 1993 *Nature* **363** 605
[3] Thess *et al* 1996 *Science* **273** 483
[4] Hone J, Whitney M, Piskoti C and Zettl A 1999 *Phys. Rev.* B **59** R2514
Hone J, Llaguno M C, Nemes N M, Johnson A T, Fisher J E, Walters D A, Casavant M J, Schmidt J and Smalley R E 2000 *Appl. Phys. Lett.* **77** 666
Yi W, Lu L, Zhang D-L, Pan Z W and Xie S S 1999 *Phys. Rev.* B **59** R9015
[5] Tersoff J 1988 *Phys. Rev. Lett.* **61** 2879
Brenner D W 1990 *Phys. Rev.* B **42** 9458
[6] Muller-Plath F 1997 *J. Chem. Phys.* **106** 6082
[7] Benedict L X, Louie S T and Cohn M L 1996 *Solid State Commun.* 100
Benedict L X, Louie S T and Cohn M L 1996 *Solid State Commun.* 177
[8] Osman M A and Srivastava D 2000 in preparation
[9] Hooker C N, Ubbelohde A R and Young D A 1963 *PRS* **276** 83
[10] Holland M G, Klein C A and Straub W D 1975 *J. Phys. Chem. Solids* **27** 903
[11] See for example Dresselhaus M, Dresselhaus G and Eklund P C 1996 *Fullerenes and Carbon Nanotubes* (San Diego, CA: Academic)
[12] Heremans J, Rahim I and Dresselhaus M S 1985 *Phys. Rev.* B **32** 2742
[13] Berman R 1976 *Thermal Conduction in Solids* (Oxford: Oxford University Press)
[14] Charlier A, McRae E, Charlier M F, Spine A and Forster S 1998 *Phys. Rev.* B **57** 6689
[15] Rao A M, Bandow S, Richter E and Eklund P C 1998 *Thin Solid Films* **331** 141
[16] Kelly B T 1981 *Physics of Graphite* (Englewood Cliffs, NJ: Applied Science) p 249
[17] Che J, Cagin T and Goddard W A III 2000 *Nanotechnology* **11** 65